IOPscience iopscience.iop.org

Home Search Collections Journals About Contact us My IOPscience

Non-classical behaviour in an $S = 5/2$ chain with next nearest neighbour interactions observed from the inelastic neutron scattering of $Mn_2(OD)_2(C_4O_4)$

This article has been downloaded from IOPscience. Please scroll down to see the full text article.

2009 J. Phys.: Condens. Matter 21 076003

(http://iopscience.iop.org/0953-8984/21/7/076003)

View the table of contents for this issue, or go to the journal homepage for more

Download details:
IP Address: 129.252.86.83
The article was downloaded on 29/05/2010 at 17:56

Please note that terms and conditions apply.

J. Phys.: Condens. Matter **21** (2009) 076003 (7pp) doi:10.1088/0953-8984/21/7/076003

Non-classical behaviour in an $S = 5/2$ chain with next nearest neighbour interactions observed from the inelastic neutron scattering of $Mn_2(OD)_2(C_4O_4)$

Richard A Mole[1,2], **John A Stride**[3], **Tobias Unruh**[2] **and Paul T Wood**[1,4]

[1] University Chemical Laboratory, Lensfield Road, Cambridge CB2 1EW, UK
[2] Forschungsneutronenquelle Heniz Maier-Leibnitz (FRM II), Technische Universität München, Lichtenbergstraße 1, 85747 Garching, Germany
[3] School of Chemistry, University of New South Wales, Anzac Parade, Kensington, Sydney NSW 2052, Australia

E-mail: ptw22@cam.ac.uk

Received 1 August 2008, in final form 12 December 2008
Published 29 January 2009
Online at stacks.iop.org/JPhysCM/21/076003

Abstract
Low-dimensional and frustrated magnetic systems often show interesting quantum phenomena. The use of large moments such as $S = 5/2$ within such materials is uncommon, partly due to the evidence that the large manifold of states associated with these centres results in pseudo-classical behaviour. Here we report on the inelastic neutron scattering of $Mn_2(OD)_2(C_4O_4)$, a well-isolated chain with next nearest neighbour interactions. We observe a magnetic excitation spectrum below 30 K whose characteristics resemble those of quantum spin singlets. Inelastic neutron scattering from a powdered sample is shown to yield a great deal of information about the nature of these effects.

(Some figures in this article are in colour only in the electronic version)

One-dimensional magnetic materials have been the subject of much experimental and theoretical discussion. It is now well established that a one-dimensional system does not undergo ordering above 0 K [1], as any long range order is destroyed by quantum fluctuations within the chain. However, long range ordering has being obtained experimentally as a result of interchain coupling and lattice distortions [2]. More recent work has concentrated on looking at more exotic chains such as integer spin systems [3], ladders [4], alternating chains [5] and those with next nearest neighbour interactions [6]—much of this has focused around the realization that these systems may show gapped excitations, as predicted by the Haldane conjecture [7]. The most frequently studied systems are those based around $S = 1/2$ and 1 ions. Larger spin systems, such as the $S = 5/2$ Mn^{2+} ion have not been studied in detail due to the lack of theoretical work—partly due to the size of the exchange matrices involved. Fisher [8] proposed the use of scaled classical spin vectors. Although this has produced good results for bulk static properties such as magnetic susceptibility, this approach fails to adequately describe the microscopic behaviour of systems. To date, most inelastic neutron scattering (INS) reported on $S = 5/2$ systems has concluded that large S results in classical behaviour [9]. Further work looking at $S = 3/2$ systems has reported quantum behaviour and suggested that the crossover from quantum to classical occurs at this value of S and as a function of temperature [10].

The use of (organic) molecular components in a *crystal engineering* approach allows chemists to generate low-dimensional networks with many pseudo-zero [11] and one-dimensional [12] systems studied. Despite the large number of publications in this field, the fraction involving neutrons as a probe for the magnetic behaviour is relatively small. This is due to the requirement of relatively large samples and the need for deuteration.

[4] Author to whom any correspondence should be addressed.

 © 2009 IOP Publishing Ltd Printed in the UK

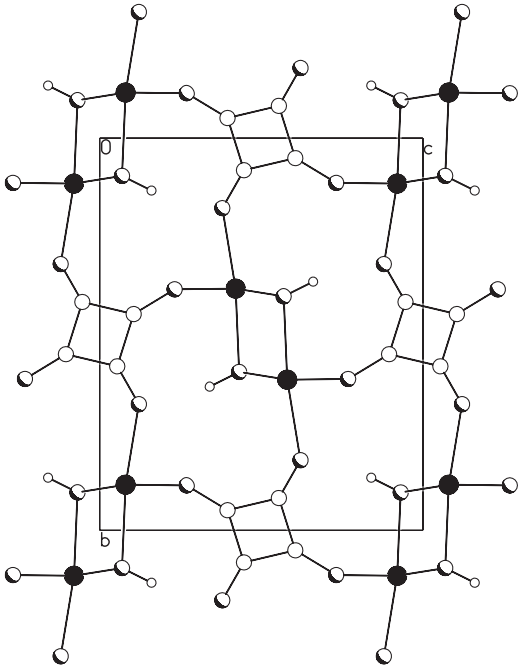

Figure 1. Projection along the a-axis showing the separation of chains. The chains run into the plane of the diagram, with Mn atoms solid, C unfilled, oxygen shaded and hydrogen small unfilled.

Here we report on our further findings, principally from inelastic neutron scattering on the low-dimensional magnetic insulator $Mn_2(OH)_2(C_4O_4)$. The crystal structure of $Mn_2(OH)_2(C_4O_4)$ has been reported previously [13]. $Mn_2(OH)_2(C_4O_4)$ crystallizes in the space group $P2_1/c$, with one Mn(II) ion, one hydroxide anion and half a squarate dianion in the asymmetric unit. The squarate dianion has two different coordination modes: a μ_2-bridging and a terminal mode. Each octahedral Mn has two μ_2-bridges and one terminal squarate. The three remaining positions are all μ_3-bridging hydroxide anions. There is a large deviation from octahedral symmetry with the most distorted angle being 79.11(4)° due to the steric requirements of the terminal squarate mode. The extended structure of $Mn_2(OH)_2(C_4O_4)$ is based around a well-isolated chain of edge-sharing hydroxide-bridged triangles propagating along the crystallographic a axis. The low symmetry of the lattice results in all triangles being scalene with the Mn–O distances being in the range 2.1133(8)–2.3654(9) Å and Mn–O–Mn angles in the range 95.73(4)°–105.44(4)°. Each squarate dianion is coordinated to four chains resulting in an interchain separation of 6.688(2) Å (figure 1). Exchange mediated by the squarate bridging ligand is thought to be very weak [14], consequently the behaviour is expected to be that of a pseudo-one-dimensional chain. The overall topology can be described as a zigzag ladder or chain with frustrating next nearest neighbour interactions (figure 2) and is described by the Hamiltonian $\hat{H} = -2\sum_i J S_{1,i} \cdot S_{2,i} + J_1 S_{1,i} \cdot S_{2,i+1} + J_2(S_{1,i} \cdot S_{1,i+1} + S_{2,i} \cdot S_{2,i+1})$. This topology has been studied extensively for the $S = 1/2$ case and the Hamiltonian can be used to describe the limiting situations of isolated chains, spin dimers, spin ladders and most importantly the frustrated chain. Several key values of J, J_1 and J_2 have been studied. Haldane [15] predicted that the exact ground state will become doubly degenerate when J_2 is weak. The nature of these ground states is exactly known at the Majumdar–Ghosh point [16] when $J = J_1 = 2J_2$ and can be described as decoupled singlets. As $J_2 \to J$ the nature of the ground state becomes more complex with incommensurate oscillations appearing in the short range correlations [17]. There are several reports of possible model systems for this topology, with varying values of J, J_1 and J_2 [18].

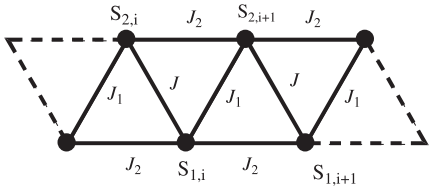

Figure 2. Suggested exchange topology for $Mn_2(OD)_2(C_4O_4)$.

The magnetic structure has been determined using neutron diffraction experiments [19] which show that long range order occurs at 12 K. The structure is unusual in that although the system consists of octahedrally coordinated high spin Mn^{2+} ions, generally considered to be Heisenberg spins, the moments align along a specific axis, indicating Ising-like behaviour. Previously we have ascribed the source of this anisotropy to the distortion of the coordination environment away from perfect O_h symmetry; as this is small, the Ising behaviour is believed to be weak, however interpretation of the INS data presented here allows us to show that it may be a consequence of the valence bond state. Single crystal x-ray diffraction has been performed both above and below the transition temperature [13], showing that there is no structural change associated with this transition. This precludes the possibility of long range order arising from instabilities due to coupling to the three-dimensional phonon field, as is the case in spin Peierls compounds [20]. The neutron diffraction data [19] shows a strong temperature dependence in the diffuse scattering component, which evolves below 50 K which we ascribe to short range ordering. Given the lack of accurate susceptibility data for this compound arising from the presence of the impurity phase $MnCO_3$, we have also performed MuSR experiments [21], which show a deviation from linear behaviour between 12.5 and 50 K. We ascribed this to the occurrence of diffuse scattering thought to be due to some sort of cooperative paramagnetism. Inelastic neutron scattering is an ideal probe of this magnetic diffuse scattering and cooperative paramagnetism.

It has so far not proved possible to prepare crystals of $Mn_2(OH)_2(C_4O_4)$ of a sufficient volume for single crystal inelastic neutron scattering measurements; however several experiments have demonstrated that neutron scattering experiments on polycrystalline samples of one-dimensional materials can yield considerable information [22]. This is particularly true when using time-of-flight spectrometers, which can simultaneously access a large region of reciprocal space and energy transfer $(\mathbf{Q}, \omega)$. The powder average of the structure factor observed experimentally is given by (1).

$$S(Q,\omega) = T(\omega)|F(Q)|^2 \frac{1}{4\pi\, Q^2} \int_{\mathbf{Q}=\mathbf{q}+\mathbf{q}_p} S(\mathbf{Q},\omega)\, \mathrm{d}\mathbf{Q} \quad (1)$$

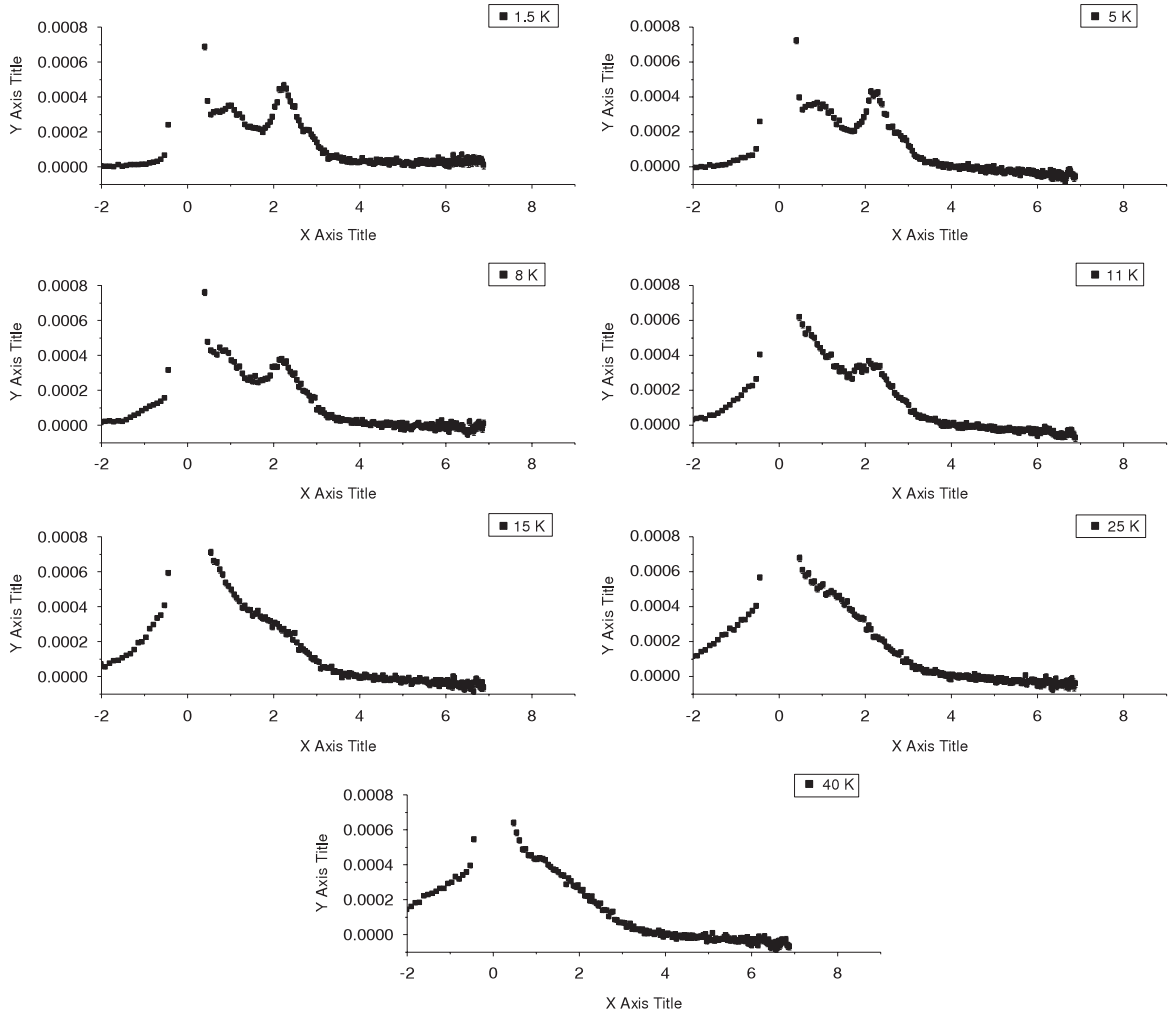

Figure 3. Cuts of the INS data obtained with $E_i = 9.7$ meV. Between $Q = 0.5$ and 1.5 Å^{-1}.

where $T(\omega)$ is the temperature factor $T(\omega) = [1 - \exp(-\hbar\omega/k_BT)]^{-1}$, $F(Q)$ is the ionic form factor and $\mathbf{q}$ and $\mathbf{q}_p$ are the parallel and perpendicular projections of the total momentum transfer $\mathbf{Q}$ relative to the chain axis.

INS measurements were performed using the IN4 spectrometer at the Institute Laue Langevin, Grenoble, France (ILL) with $E_i = 9.7$ and 6.3 meV and energy transfer up to 5 meV, with a resolution of 335 μeV or 190 μeV respectively at the elastic line, and with the TofTof spectrometer [23] at the Garching research reactor (FRM-II), Munich, Germany, with $E_i = 5.7$ meV and a corresponding resolution of 150 μeV. The sample was placed in a hollow cylindrical aluminium can and data were recorded at a range of temperatures between 1.5 and 40 K. The raw data were treated by subtracting the scattering from an empty can and normalizing to a vanadium scan. Standard data treatments have been performed within the LAMP [24] and IDA programmes [25].

Initially we will discuss the data integrated over the region $Q = 0.5$ to 1.5 Å^{-1}. This is the region where we anticipate magnetic excitations and where any excitations due to phonons etc will be very weak (figure 3). At base temperature two excitations are observed, the first is centred on 1.2 meV, the second 2.2 meV. Upon heating to 5 and then 8 K the excitation at 2.2 meV remains the same with slight changes in intensity. The maximum in the low energy mode shifts to lower energies; at 11 K, the low energy mode no longer shows a distinct maximum that is well resolved from the elastic line. Data collected at 11 and 13 K show very little change in the inelastic response, while absence of the contribution of magnetic Bragg peaks from the elastic line show that the system no longer displays long range magnetic order (figure 4). Data collected at 15 K, well above the magnetic phase transition, shows that the high energy peak is still present. However this is now much broader and appears as a shoulder on the lower energy excitation. Data collected at 25 and 40 K shows no evidence of this high energy excitation, with the low energy excitation now very broad.

Data collected simultaneously across the full angular range of the detector using an incident energy of 9.7 meV were combined to produce contour plots of the scattering intensity (figure 5), allowing us to study the detailed nature of the Q dependence of the excitations described above. At 40 K, excitations extend across the entire Q range with an increased density of states in the range 1 Å^{-1} $< Q <$ 1.5 Å^{-1}. At lower temperatures there are fewer occupied states in the region $Q <$ 1 Å^{-1} and a sharp increase in intensity at this point.

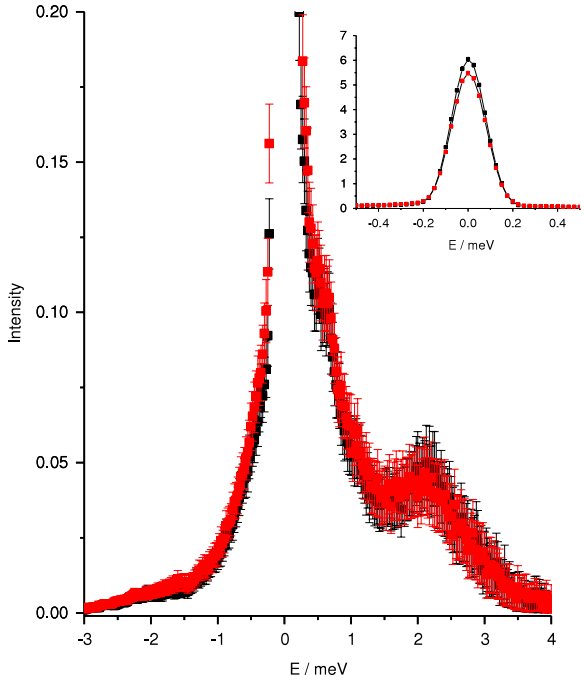

Figure 4. Data collected at 11 K (upper, black) and 13 K (lower, red) using the time of flight spectrometer TofTof. This clearly shows that the gapped mode does not change significantly on the transition to long range order. Inset: the elastic line in the same measurement, clearly showing extra intensity at 11 K due to the formation of magnetic Bragg peaks.

The low energy mode shows dispersion in the measurements obtained at 1.5 and 5 K, with excitations meeting the elastic line at $Q = 1$ and 1.35 Å^{-1}. At the lowest temperatures the high energy mode is clearly visible, this second excitation shows dispersion below $Q = 1$ Å^{-1}, whereas above $Q = 1$ Å^{-1} the excitation shows no variation with Q. The point $Q = 1$ Å^{-1} is important as this point corresponds to the edge of the first Brillouin zone in a perfectly one-dimensional system. Due to the lack of intensity in the low energy mode in the region below $Q = 1$ Å^{-1}, we can examine the temperature dependence of only the high energy mode; integrations in the region 0.5 Å^{-1} $< Q <$ 1 Å^{-1} were performed and clearly show the formation of a gapped excitation above T_N (figure 6).

1. Analysis

First we will consider the excitation spectrum at low temperature and discuss how this changes with increasing temperature. The low energy mode shows a strong dispersion at low temperature with the excitation meeting the elastic line at several positions, these positions correspond to the magnetic Bragg peaks, thus identifying this low energy mode as acoustic magnons of the Néel phase. A second point of note is that the magnon modes display a strong dispersion above $Q = 1$ Å^{-1}, despite this being the edge of the first Brillouin zone, where normally in powder data one would expect to see a continuum of excitations as a feature of the powder averaging. In the case of $Mn_2(OD)_2(C_4O_4)$ we

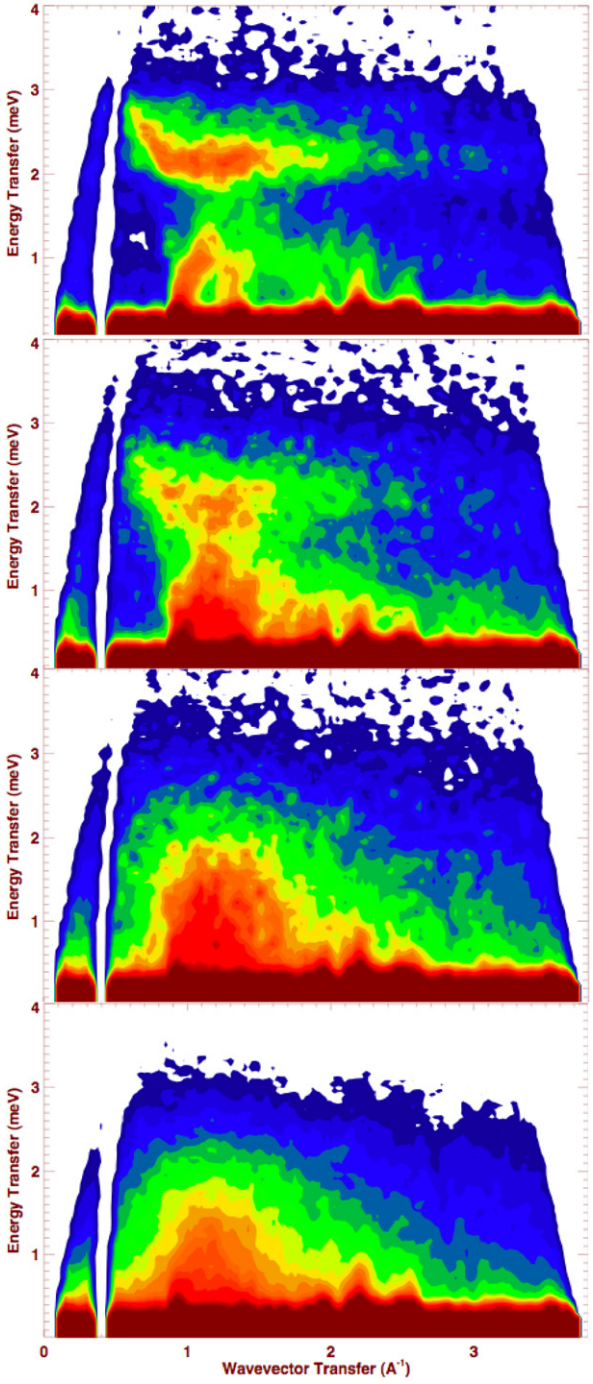

Figure 5. False colour plots of the inelastic neutron scattering data at $T = 5$, 12, 20 and 40 K (top to bottom) as measured on IN4 with $E_i = 9.7$ meV.

believe that we continue to see dispersion beyond the zone boundary due to the highly one dimension nature of the magnetic exchange topology, consequently the powder average is strongly dispersive throughout reciprocal space. There is no model for a next nearest neighbour chain with interchain interactions, preventing full characterization of this mode.

Next we will consider the high energy or optic mode. The Q-dependence of this mode strongly resembles the form factor dependence of a spin dimer [26]. If the Ising spin anisotropy is

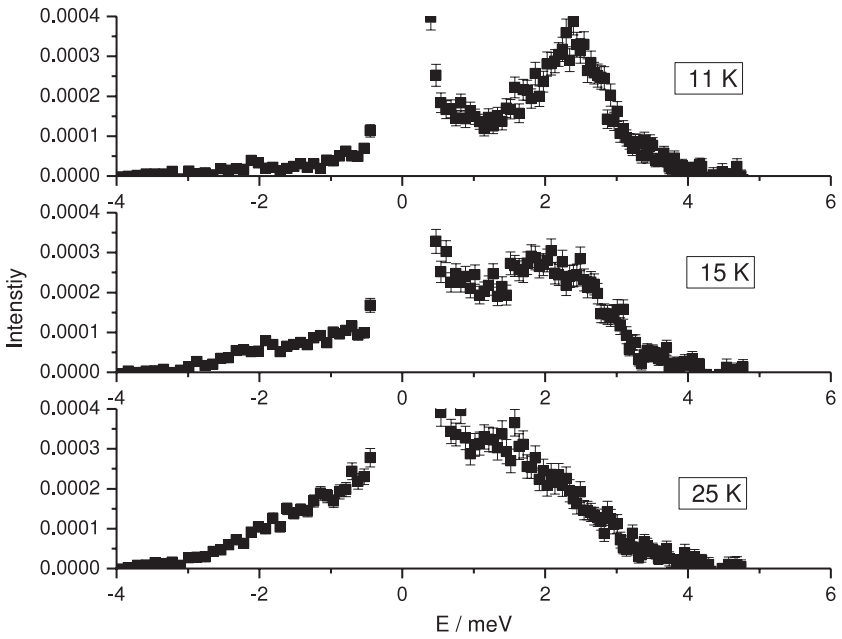

Figure 6. Evolution of the gapped peak excitation with temperature in the region 0.5 Å^{-1} < Q < 1 Å^{-1}. The peak is clearly visible at 15 K, well above T_N.

suitably small, the nature of this excitation can be considered in a model independent analysis; i.e. by assuming the moments to be isotropic, the system obeys the simple Hamiltonian given in (2),

$$\hat{H} = \tfrac{1}{2}\sum_{r,\mathbf{d}} J_{\mathbf{d}} S_r \cdot S_{r+\mathbf{d}}. \tag{2}$$

Applying the constraints due to the sum rules [27], we can write the scattering function as

$$S(Q) \equiv \hbar^2 \int_{-\infty}^{\infty} \omega S^{\alpha\alpha}(\mathbf{Q},\omega)\,\mathrm{d}\omega$$
$$= -\frac{1}{3}\frac{1}{N}\sum_{r,\mathbf{d}} J_{\mathbf{d}}\langle S_r \cdot S_{r+\mathbf{d}}\rangle(1-\cos(\mathbf{Q}\cdot\mathbf{d})) \tag{3}$$

where the sum over **d** is the set of all bond vectors connecting a spin to its neighbours, $J_{\mathbf{d}}$ is the associated exchange interaction and r runs over all N spins. Taking the spherical average we obtain

$$S(Q) \equiv \hbar^2 \int_{-\infty}^{\infty} \omega \tilde{I}_m(Q,\hbar\omega)\,\mathrm{d}\omega$$
$$= -\frac{2}{3}\left|\frac{g}{2}f(Q)\right|^2 \frac{1}{N}\sum_{r,\mathbf{d}} J_{\mathbf{d}}\langle S_r \cdot S_{r+\mathbf{d}}\rangle\left(1-\frac{\sin Qd}{Qd}\right), \tag{4}$$

where $f(Q)$ is the magnetic form factor of Mn^{2+}; the empirical form for an isotropic $S = 5/2$ is given by Brown [28].

Cross-sections summed over the entire width of the excitation (2.2 ± 0.1 meV) were taken and fits made to this model (figure 7). To a first approximation the strongest exchange interactions are those mediated by the hydroxide-bridged chain. Consequently initial refinements of the data included only one interaction parameter and one distance; **d** and $J_{\mathbf{d}}$. This yielded a Mn–Mn distance of 3.3(1) Å, in reasonable agreement with the crystallographically determined Mn–Mn distances of 3.2370(8) (rung), 3.1974(8) (rung) and

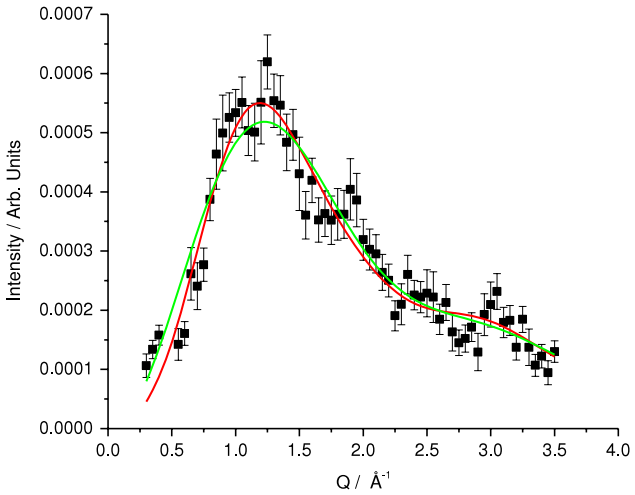

Figure 7. Constant energy cross section at 2.2(1) meV from the $T = 1.5$ K with $E_i = 9.7$ meV. The solid lines are the fits described in the text. The green (lower) line involves only one exchange interaction and the red (upper) two.

3.3760(8) Å (rail). Although all these refinements favour an interaction length of approximately 3.3 Å, it is not possible to assign the strongest interaction as this would require refinement of three interaction distances resulting in over parameterization.

The two parameter, nearest neighbour model gives a relatively good fit to the data. Any deviations from this model can be ascribed to the fact that at low temperatures this is a long range ordered state and there will be interchain interactions, as a result of long range ordering and hence exchange interactions in more than one direction. Attempts to rationalize the data on the basis of a second exchange interaction can lead to

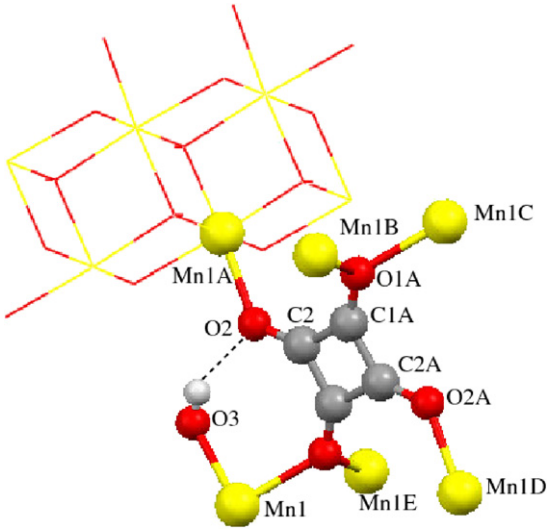

Figure 8. Squarate dianion with all its associated Mn ions is shown in the ball and stick section. The wire frame component shows how this relates to the rest of the chain structure. Finally the dashed black line shows a potential hydrogen bonding pathway.

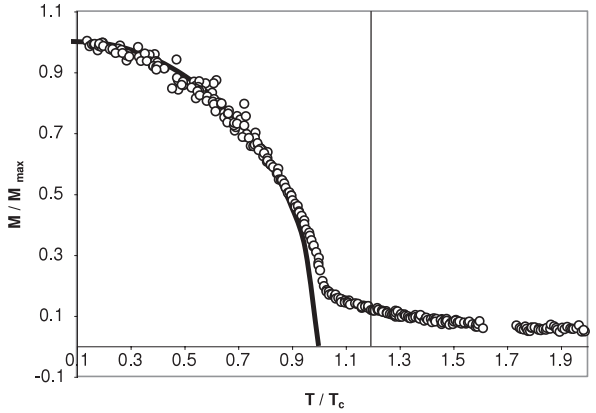

Figure 9. Integrated intensity over the (2 0 0) magnetic Bragg peak (open circles determined by neutron diffraction) in normalized units. The solid line is a fit to the ideal spontaneous magnetization for an $S = 5/2$ system, with $T_c = 12.5$ K. The vertical line at $T/T_c = 1.2$ indicates 15 K, where the high energy, excitation is still observed.

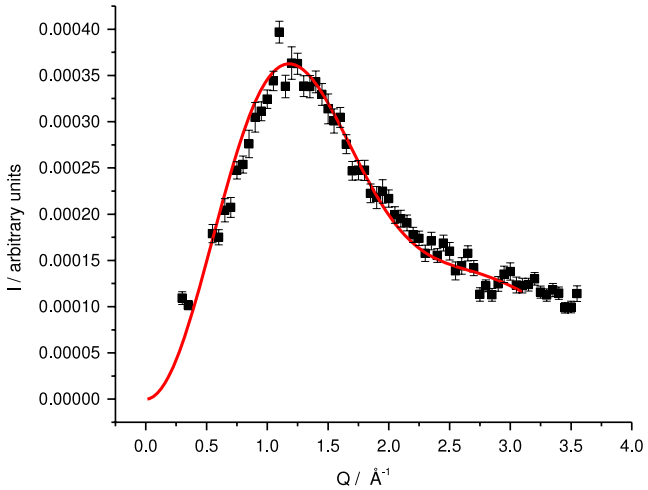

Figure 10. Integral over the energy range $E = 2.2(1)$ meV on data recorded at 15 K. The fit is the pairwise interactions over a distance of 3.3 Å.

better fits, the data were again fitted to (4) using two terms in the summation (figure 7). The values of $\mathbf{d}_1$, $\mathbf{d}_2$, $J_{\mathbf{d}1}/J_{\mathbf{d}2}$ were 3.36(6) Å, 6.7(7) Å and −6.3(3) for the 5 K data. The negative ratio indicates that the second interaction is opposite in sign (ferromagnetic) and significantly weaker than the nearest neighbour term. Using these values gives a better description of the low Q data, but $J_{\mathbf{d}2}$ typically refines to a value so small that no modulation of intensity at high Q is predicted, consequently although all the long range Mn–Mn distances are known from the crystal structure (figure 8), it is not possible to ascribe this second interaction length to any one Mn–Mn vector, due to this lack of intensity modulation. The real situation is that there are probably multiple long range interactions that give rise to the observed Q dependence however these cannot be accounted for due to the weak nature of these interactions and the loss of information that occurs on powder averaging.

One of the interesting features of this system is that this high energy mode is still present above the Néel temperature. This reveals that it cannot just be a simple magnon mode of the Néel phase—as this would no longer be present above T_N and certainly would not be anticipated well above the critical region (figure 9). Analysis of the Q dependence of this mode at 15 K shows that the interaction is now very well described by a pairwise interaction between spins (figure 10). Given this Q dependence we believe that we can assign this excitation to a singlet triplet excitation as predicted in a valence bond solid [29].

At 25 K there is no longer any evidence of the high energy excitation. Summing the data over the entire inelastic region shows that the Q dependence can be well described by the singlet triplet excitations due to pairwise interactions between spins (figure 11). Given that this is summing over a gapless continuum of states, we have ascribed this to be a valence bond liquid. Finally At 40 K the observed excitation is weaker, indicating that the system is tending towards a conventional paramagnetic state.

Essentially, we have interpreted the data as follows. At high temperature we anticipate the system to be a conventional paramagnet, below 50 K, the system becomes a cooperative paramagnet and shows liquid-like behaviour. Below 25 K, there is a partial freezing of this liquid state and we observe gapped excitations associated with a valence bond solid. Upon cooling to 12.5 K long range order is achieved, however the excitations maintain a highly one-dimensional character.

Given the analysis above we will now return to the magnetic structure determined previously and reinterpret our results. It was noted in the original work that the magnetic structure depends on two irreducible representations that are related by anti-unitary symmetry and belong to the same irreducible co-representation. These structures can be interpreted as the doubly degenerate prediction of the Majumdar–Ghosh and Haldane models, though these are

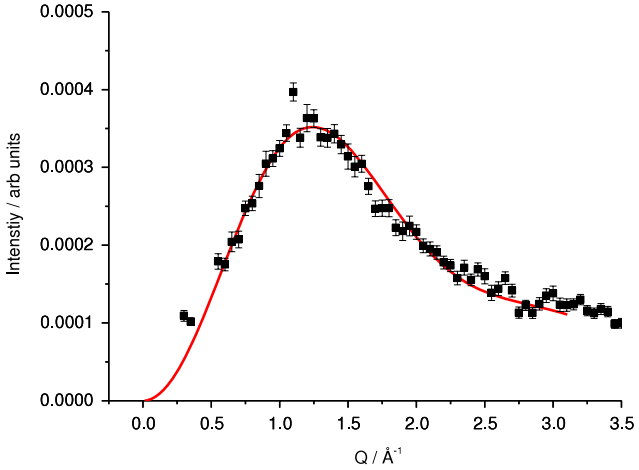

Figure 11. Integration of the 25 K data over the entire inelastic excitation. The red line is a fit assuming pairwise coupling of the spins, with an average interaction length of 3.3 Å.

stabilized by interchain interactions resulting in long range order. Both of these models predict gapped excitations. Recent work on the pyrochlore systems Y_2RuO_7 [30] and $Zn_xCu_{4-x}(OD)_6Cl_2$ [31], have shown that the observation of a collinear structure can also be a feature of highly frustrated systems, where the valence bond state is also predicted. If this is a valence bond state that arises from the inequivalence of exchange interactions along the chain, the valence bond singlets would form around the dominant interactions and the excitations correspond to promoting one of these into the triplet state. On further cooling, the spins freeze into a collinear Néel state rather than the non-collinear arrangements thought to minimize the energy of a frustrated state and observed for example in the kagome antiferromagnets [32] and the spiral ground states of the spinels [33].

2. Conclusions

The inelastic neutron scattering from $Mn_2(OH)_2(C_4O_4)$ reveals a rich phase diagram. At high temperatures the scattering is dominated by short range ordering and shows behaviour characteristic of a spin liquid, at intermediate temperatures well below the Weiss temperature yet above T_N, we have shown evidence of a valence bond solid with triplet excitations. This valence bond solid appears to coexist with the liquid state, indicating that the freezing of the liquid is not a sharp transition. At the Néel point, interchain interactions become dominant resulting in long range ordering. Even with the amount of data available from powder averaging versus single crystal data, analysis of the Q dependence has allowed us to show that the interchain interactions are very weak and the nature of the magnon modes is still thought to be highly one-dimensional as seen in the observed dispersion. Ideally one should analyse the data using a powder average of the structure factor, however the dispersion relation for an $S = 5/2$ chain with next nearest neighbour interactions is not well established, so this degree of analysis cannot be performed. All analyses indicate that this system is an $S = 5/2$ system showing quantum behaviour. To the best of the authors' knowledge this has not previously been observed for systems having large S values. The reason for the departure from the classical behaviour normally observed in such systems is that the energy scales are lowered by two mechanisms, firstly the low-dimensional nature of the system and secondly the geometric frustration.

Acknowledgments

The authors would like to thank H Mutka (ILL) for helpful discussions, the EPSRC (RAM) for funding and the ILL for technical support.

References

[1] Bethe H A 1931 *Z. Phys.* **71** 205
[2] Hase M, Terasaki I and Uchinokura K 1993 *Phys. Rev. Lett.* **70** 3651
[3] Morra R M *et al* 1998 *Phys. Rev.* B **38** 543
[4] Barnes T *et al* 1993 *Phys. Rev.* B **47** 3196
[5] Barnes T, Riera J and Tennant D A 1999 *Phys. Rev.* B **59** 11384
[6] Oosawa A *et al* 2002 *Phys. Rev.* B **65** 094426
[7] Haldane F D M 1983 *Phys. Rev. Lett.* **50** 1153
[8] Fisher M E 1964 *Am. J. Phys.* **32** 343
[9] Hutchings M T *et al* 1972 *Phys. Rev.* B **5** 1999
[10] Itoh S H *et al* 1999 *Phys. Rev.* B **59** 14406
[11] Sessoli R *et al* 1993 *Nature* **365** 141
[12] Humphery S M *et al* 2004 *Dalton Trans.* 1670–8
[13] Yufit D S *et al* 1999 *Chem. Commun.* 1561
[14] Castro I *et al* 1995 *Inorg. Chem.* **34** 4903
[15] Haldane F D M 1982 *Phys. Rev.* B **25** 4925
[16] Maumdar C K and Ghosh D K 1969 *J. Math. Phys.* **10** 1388
[17] White S R and Affleck I 1996 *Phys. Rev.* B **54** 9862
[18] Tsirlin A A, Nath R, Geibel C and Rosner H 2008 *Phys. Rev.* B **77** 104436
[19] Mole R A *et al* 2006 *Physica* B **385/386** 435
[20] Pouget J P *et al* 1994 *Phys. Rev. Lett.* **72** 4037
[21] Mole R A, Stride J A, Cottrell S P and Wood P T 2008 *Inorg. Chim. Acta* **361** 3718
[22] Mutka H *et al* 1991 *Phys. Rev. Lett.* **67** 497
[23] Unruh T, Neuhaus J and Petry W 2007 *Nucl. Instrum. Methods* A **580** 1414
[24] *LAMP The Large Array Manipulation Program* http://www.ill.fr/data_treat/lamp/front.html
[25] *IDA Interactive Data Analysis* http://iffwww.iff.kfa-juelich.de/~wuttke/frida2.git/
[26] Furrer A and Güdel H U 1997 *Phys. Rev. Lett.* **39** 657
[27] Hammar P R, Reich D H and Broholm C 1998 *Phys. Rev.* B **57** 7846
[28] Brown P J 1995 *International Tables of Crystallography* vol C, ed A J C Wilson (London: Kluwer–Academic)
[29] Sachdev S 2008 *Nat. Phys.* **4** 173
[30] Van Dujin J, Hur N, Taylor J W, Qui Y, Huang Q Z, Cheong S-W, Broholm C and Perring T G 2008 *Phys. Rev.* B **77** 020405
[31] Lee S–H, Kikuchi H, Qiu Y, Lake B, Huang Q, Habicht K and Kiefer K 2007 *Nat. Mater.* **6** 852
[32] Yildirim T and Harris A B 2006 *Phys. Rev.* B **73** 214446
[33] Krimmel A, Mücksch M, Turksan V, Koza M M, Mutka H, Ritter C, Sheptyakov D V, Horn S and Loidl A 2006 *Phys. Rev.* B **73** 014413